

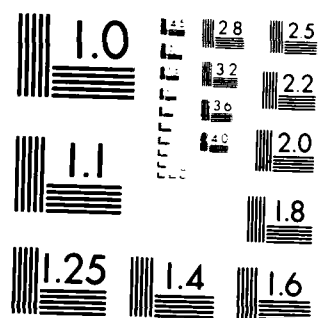
THE SOLAR RADIATION FIELD AT TWILIGHT BELOW 100 KM: A SPHERICAL MODEL(U) NAVAL RESEARCH LAB WASHINGTON DC E O HULBURT CENTER FOR SPACE.. D E ANDERSON MAY 82 1/1

FAA/EE-82-18 DTFA01-81-Y-10512

F/G 3/2

NL

END
DATE
FILMED
88-1-1
DTIC



MICROCOPY RESOLUTION TEST CHART
NATIONAL BUREAU OF STANDARDS-1963-A

17



US Department
of Transportation
Federal Aviation
Administration

The Solar Radiation Field at Twilight Below 100 KM: A Spherical Model

Office of Environment
and Energy
Washington, DC 20591

AD A122832

DTIC
ELECTE
DEC 28 1982
S D
E

FILE COPY

Donald E. Anderson, Jr.

May 1982

This document has been approved
for public release and sales its
distribution is unlimited.

82 12 28 016

Technical Report Documentation Page

1. Report No. FAA-EE-82-18	2. Government Accession No. AD A122 832	3. Recipient's Catalog No.
4. Title and Subtitle The Solar Radiation Field at Twilight below 100 Km: A Spherical Model	5. Report Date May 1982	6. Performing Organization Code
7. Author(s) Donald E. Anderson, Jr.	8. Performing Organization Report No.	
9. Performing Organization Name and Address Naval Research Laboratory 4555 Overlook Avenue, S.W. Washington, D.C. 20375	10. Work Unit No. TRAIS:	
12. Sponsoring Agency Name and Address Department of Transportation Federal Aviation Administration Office of Environment and Energy Air Quality Division Washington, D.C. 20591	11. Contract or Grant No. DTFA01-81-Y-10512	
15. Supplementary Notes	13. Type of Report and Period Covered Final Report	14. Sponsoring Agency Code
16. Abstract <p>Time dependent calculations of minor species distributions require as input the solar radiation field as a function of altitude and solar zenith angle. An isotropic spherical model of the radiation field has been developed to determine the solar radiation field in twilight. Comparison of the spherical model with a plane parallel model of the multiple scattering of radiation at twilight shows that: (1) for solar zenith angles less than 95°, plane parallel solutions are suitable if the initial deposition of solar energy is calculated for a spherical atmosphere; (2) for solar zenith angles greater than 95°, the plane parallel radiation field is several orders of magnitude smaller than that calculated with the spherical model; (3) at altitudes above 40 km, the spherical model predicts 10 - 20 % less radiation than the radiation field calculated with the plane parallel model.</p>		
17. Key Words Troposphere, Stratosphere, Solar Radiation, Twilight, Multiple Scattering	18. Distribution Statement This document is available to the public through the National Technical Information Service Springfield, Virginia 22161	
19. Security Classif. (of this report) UNCLASSIFIED	20. Security Classif. (of this page) UNCLASSIFIED	21. No. of Pages 17
		22. Price

THE SOLAR RADIATION FIELD AT TWILIGHT
BELOW 100 KM: A SPHERICAL MODEL

by

Donald E. Anderson, Jr.
E. O. Hulburt Center for Space Research
Naval Research Laboratory
Washington, DC 20375

Application For	
INDEXED	<input checked="" type="checkbox"/>
SERIALIZED	<input type="checkbox"/>
FILED	<input type="checkbox"/>
APR 11 1975	
Dist	Special
A	

Abstract



Time dependent calculations of minor species distributions require as input the solar radiation field as a function of altitude and solar zenith angle. An isotropic spherical model of the radiation field has been developed to determine the solar radiation field in twilight. Comparison of the spherical model with a plane parallel model of the multiple scattering of radiation at twilight shows that: (1) for solar zenith angles less than 95° , plane parallel solutions are suitable if the initial deposition of solar energy is calculated for a spherical atmosphere; (2) for solar zenith angles greater than 95° , the plane parallel radiation field is several orders of magnitude smaller than that calculated with the spherical model; (3) at altitudes above 40 km, the spherical model predicts 10 - 20 % less radiation than the radiation field calculated with the plane parallel model.

CONTENTS

ABSTRACT.....	i
LIST OF FIGURES.....	iv
INTRODUCTION.....	1
THE MODELS.....	1
RESULTS.....	2
A. Calculation of F_0	2
B. Calculation of F	3
DISCUSSION.....	4
BIBLIOGRAPHY.....	5

LIST OF FIGURES

Figure 1. Neutral Atmosphere Density Distribution. Ozone is scaled by a factor of 100.....	7
Figure 2. O_2 and O_3 pure absorption cross sections. O_2 cross section is scaled upward by a factor of 10.....	8
Figure 3. Percent error in plane parallel F_0 when compared to spherical F_0 at $\lambda = 325$ nm and θ_0 as indicated. Dashed and solid curves are for $\tau_p = 0$ and 0.14, respectively.....	9
Figure 4. Spherical F_0 at $\lambda = 325$ nm and, θ_0 as indicated.....	10
Figure 5. F as a function of θ_0 at $\lambda = 325$ nm. Solid curves are spherical solutions, and dashed curves are plane parallel solutions. θ_0 as indicated.....	11
Figure 6. F as a function of θ_0 at $\lambda = 250$ nm. See Figure 5 caption.....	12
Figure 7. F as a function of θ_0 at $\lambda = 450$ nm. See Figure 5 caption.....	13

I. Introduction

Time dependent calculations of minor species distributions require as input the solar radiation field as a function of altitude z and solar zenith angle θ_0 . There has been some concern that results from plane parallel models may be incorrect at twilight. In the present study, an isotropic spherical model of the radiation field has been developed to address the twilight problem. The model does not include refraction effects, ground albedo, or aerosols, but does include molecular oxygen (O_2) and ozone (O_3) absorption, and multiple scattering in an inhomogeneous, spherical atmosphere. Ground albedo is relatively unimportant in twilight; refraction effects may be neglected except when making comparison to high resolution measurements; and the presence of aerosols slightly enhance the degree of multiple scattering at all wavelengths. These effects may be included at a later time but the basic results described here will not be affected.

II. The Models

The model atmosphere employed is the U.S. Standard Atmosphere (1976) with the O_3 profile from Nicolet (1978). The O_3 cross section between 200 and 800 nm is also from Nicolet (1978), as is the O_2 absorption cross section. The model atmosphere is shown in Figure 1 and the O_3 and O_2 cross sections in Figure 2.

The spherical radiative transfer model is patterned after the model developed by Anderson and Hord (1977) for calculation of resonance scattering by atomic hydrogen of the solar Lyman-alpha flux incident on planetary thermospheres and exospheres. The basic physical model for Rayleigh and Mie scattering is described for the plane parallel case by

Anderson and Meier (1979) and Meier et al., (1982). Detailed numerical results for the wavelength region 200-800 nm in the troposphere and stratosphere are described by Nicolet et al., (1982).

Briefly, both the plane parallel and spherical theory used in this study solve the integral equation of radiative transfer for the flux into a volume element F . F is normalized to the solar flux at the top of the atmosphere F_∞ , where F_∞ is in units $\text{photons cm}^{-2}\text{s}^{-1}\text{nm}^{-1}$. The plane parallel model assumes azimuthal symmetry and utilizes Chandrasekhar's (1960) E functions to reduce the problem to one dimension: namely F as function of vertical optical depth τ , or altitude. In the spherical code, azimuthal symmetry is assumed, but F is now an interlocking function of τ and θ_0 . Thus, on multiple scattering, photons are allowed to migrate in both τ and θ_0 . It will be shown below that the effects of this coupling can be very large in twilight.

III. Results

A. Calculation of F_0

When plane parallel models are employed to calculate $F(\tau, \theta_0)$, the attenuated direct flux $F_0(\tau, \theta_0)$ is usually given by

$$F_0(\tau, \theta_0) = \exp[-(\tau + \tau_p) \sec \theta_0] \quad (1)$$

τ is related in a straightforward way to z noting that

$$\tau = \sigma_s \int N(z) dz \quad (2)$$

where σ_s is the cross section for Rayleigh scattering, and N is the neutral atmosphere density at altitude z in the atmosphere. An absorption which removes a photon from further scattering is designated a pure absorption, and the pure absorption optical depth is

$$\tau_p = \int [\sigma_{O_3} N_{O_3}(z) + \sigma_{O_2} N_{O_2}(z)] dz \quad (3)$$

where the σ 's are the pure absorption cross sections. If the pure absorber is homogeneously mixed with the scatters, then Chapman functions (Smith and Smith, 1972) may be used in place of $\sec \theta_0$ in (1) to account for effects on F_0 of sphericity. Since O_3 is not homogeneously mixed neither Chapman functions, nor $\sec \theta_0$ is appropriate. Instead, the true slant optical depth must be calculated taking into account the inhomogeneities due to ozone. A comparison of (1) with the correct F_0 is shown in Figure 3 at $\theta_0 = 80, 86$, and 88° , for $\lambda = 325$ nm, $\tau_p = 0.14$ and $\lambda = 325$ nm, $\tau_p = 0$, respectively. Clearly, below 50 km, spherical effects are important for $\theta_0 > 80^\circ$. No comparisons are made for $\theta_0 \geq 90^\circ$, since the plane parallel F_0 is not defined. In Figure 4, F_0 is shown for $\lambda = 325$ nm and θ_0 from 0° to 98° . The wavelength $\lambda = 325$ nm is chosen throughout for illustrative purposes, since both pure absorption and multiple scattering effects are important. However, the model does cover the entire range 200 - 800 nm.

B. Calculation of F

Values of F at $\lambda = 325$ nm are shown in Figure 5 for $\theta_0 = 60^\circ$ to 104° . The dashed curves are the values of F calculated with the correct spherical F_0 , but the multiple scattering is assumed to take place in a plane parallel atmosphere. It is clear from Figure 5 that for $\theta_0 < 92^\circ$ the plane parallel solution with a spherical F_0 is adequate to describe the multiple scattering. However, for $\theta_0 > 96^\circ$ the plane parallel solutions are orders of magnitude lower than the spherical solutions and are off scale.

Another result, not apparent on the log plot in Figure 5, is that above 40 km, F (spherical) falls about 10 to 20% below F (plane parallel) at all θ_0 . This result has been noted before (Strickland and Anderson,

1973) and occurs because a photon emitted at a given altitude in a spherical atmosphere has a greater probability of escape from the medium than in a plane parallel atmosphere. As $z \rightarrow \infty$ the escape probability approaches 0.5 in a plane parallel medium, and 1.0 in a spherical medium.

As an example of the wavelength dependence, Figures 6 and 7 show $F(\theta_0)$ for $\lambda = 250$ and 450 nm, respectively. At short wavelengths ($\lambda < 325$ nm) ozone absorbs much of the radiation so that F is low, and is essentially zero below the ozone maximum. As λ increases beyond 350 nm F gradually decreases in proportion to the Rayleigh optical depth, and thus the multiple scattering decreases.

IV. Discussion

The purpose of this research effort was: (1) to develop a spherical model of the multiple scattering of solar radiation in the twilight atmosphere; and (2) to establish a range of validity for the use of plane parallel models in twilight. The initial model has been developed. A more sophisticated model may be developed in the future which includes such effects as refraction of sunlight, anisotropic scattering by aerosols, ground albedo, and clouds. But the result of comparison with the present model and a plane parallel model suggests that for $\theta_0 < 95^\circ$, the plane parallel solution is sufficient, if the proper F_0 is used. This conclusion is stated with the caveat that the spherical solutions are 10-20% lower than the plane parallel solutions at all θ_0 for $z > 40$ km.

For $\theta_0 > 95^\circ$ plane parallel solutions are not satisfactory, and the future improvement of the present model depends to some extent on whether or not the enormous differences in F between the two models have any effect on the photochemistry in the atmosphere below 100 km.

BIBLIOGRAPHY

- Anderson, D. E. Jr., and C. W. Hord, "Multidimensional Radiative Transfer: Applications to Planetary Coronae", Planet. Space Sci., 25, 1977.
- Anderson, D. E. Jr., and R. R. Meier, "The Effects of Anisotropic Multiple Scattering on Solar Radiation in the Troposphere and Stratosphere", Appl. Optics, 18, 1955.
- Chandrasekhar, S. "Radiative Transfer", Dover Publications, Inc. New York, New York, 1960.
- Meier, R. R., D. E. Anderson, Jr., and M. Nicolet, "Radiation Field in the Troposphere and Stratosphere: I. General Analysis", Planet. Space Sci., in press, 1982.
- Nicolet, M., "Etude des reactions chimiques de l'ozone dans la stratosphere", Institut Royal Meteorologique de Belgique, Brussels, Belgium, 1978.
- Nicolet, M., R. R. Meier, and D. E. Anderson, Jr., "Radiation Field in the Troposphere and Stratosphere: II. Numerical Analysis", Planet. Space Sci., in press, 1982.
- Smith, F. L. III., and C. Smith, "Numerical Evaluation of Chapman's Grazing Incidence $ch(X, \chi)$ ", J. Geophys. Res., 77, 3592, 1972.
- Strickland, D. J., and D. E. Anderson, Jr., "Theoretical Emergent Lyman- α Intensities From Mars", J. Geophys. Res., 78, 1973.

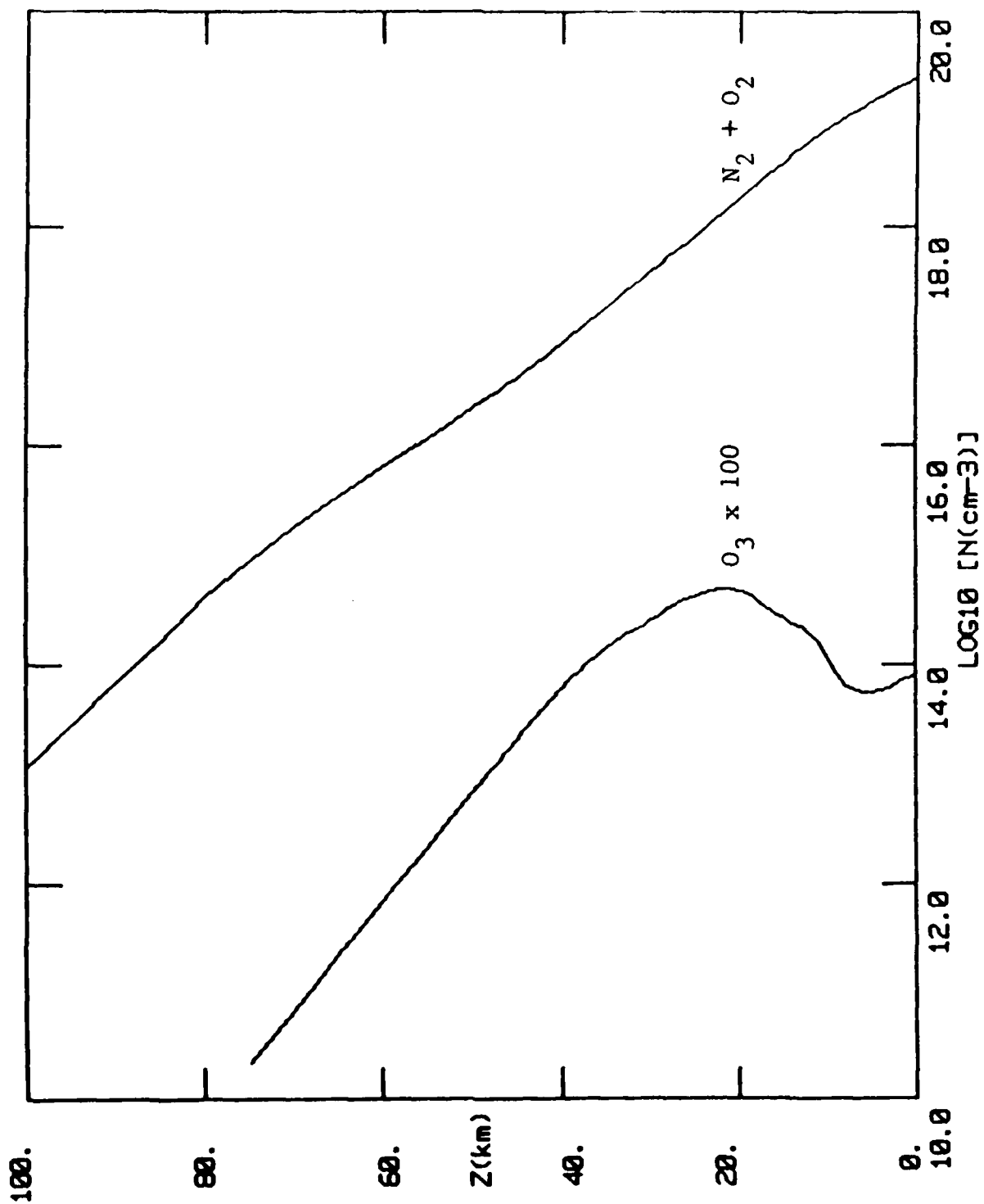


Figure 1. Neutral Atmosphere Density Distribution. Ozone is scaled by a factor of 100.

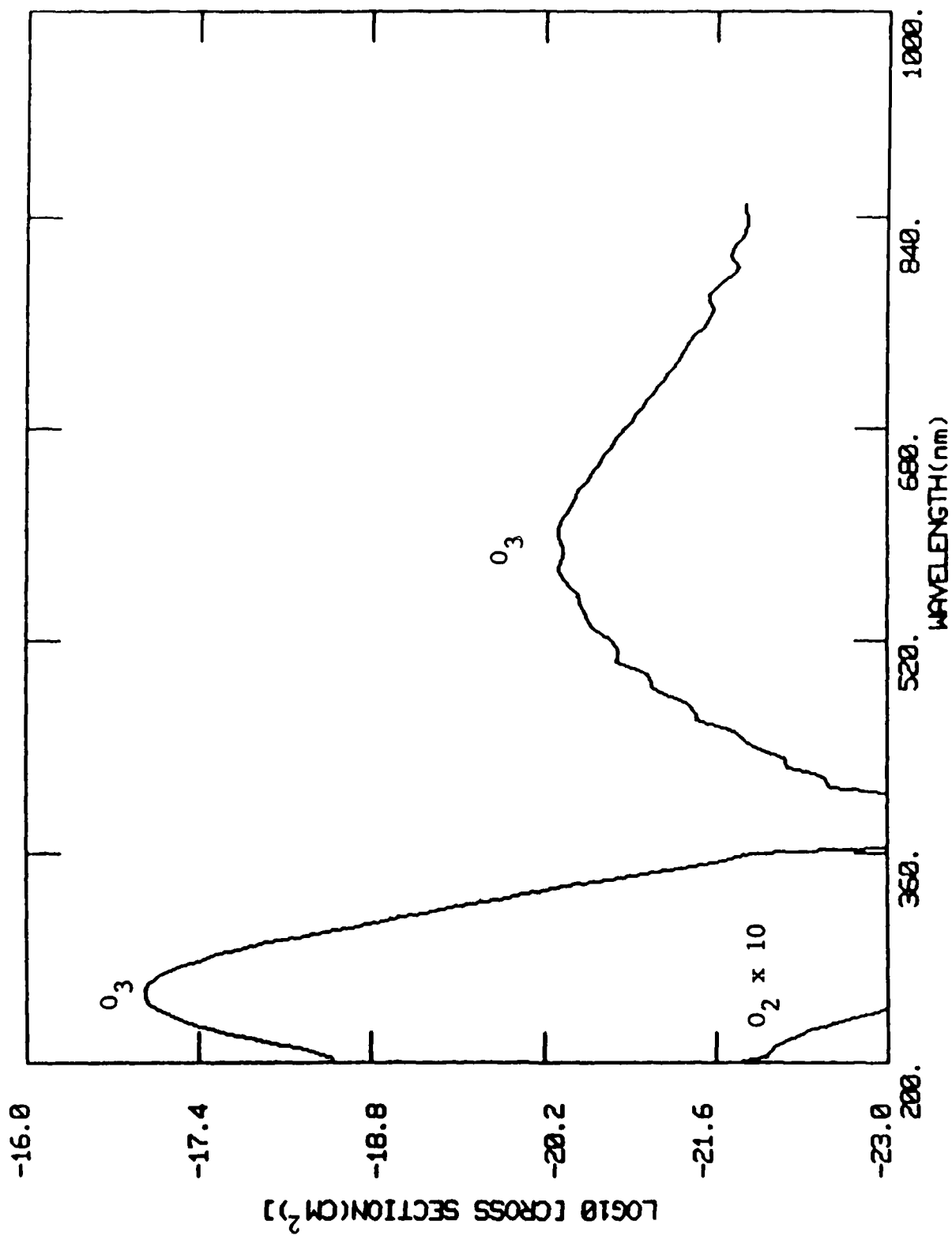


Figure 2. O₂ and O₃ pure absorption cross sections. O₂ cross section is scaled upward by a factor of 10.

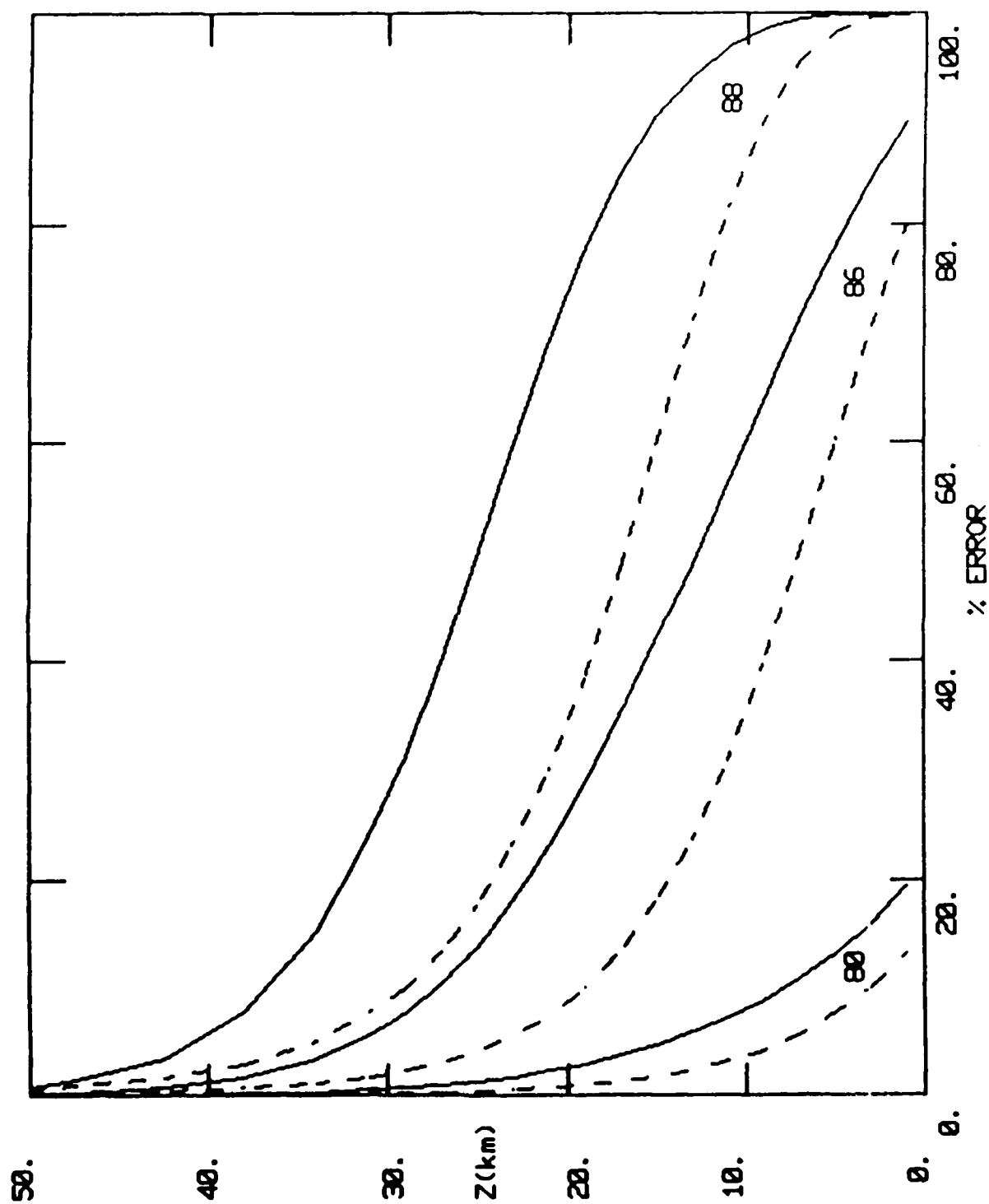


Figure 3. Percent error in plane parallel F_0 when compared to spherical F_0 at $\lambda = 325 \text{ nm}$ and O_0 as indicated. Dashed and solid curves are for $\tau_p = 0$ and 0.14 , respectively.

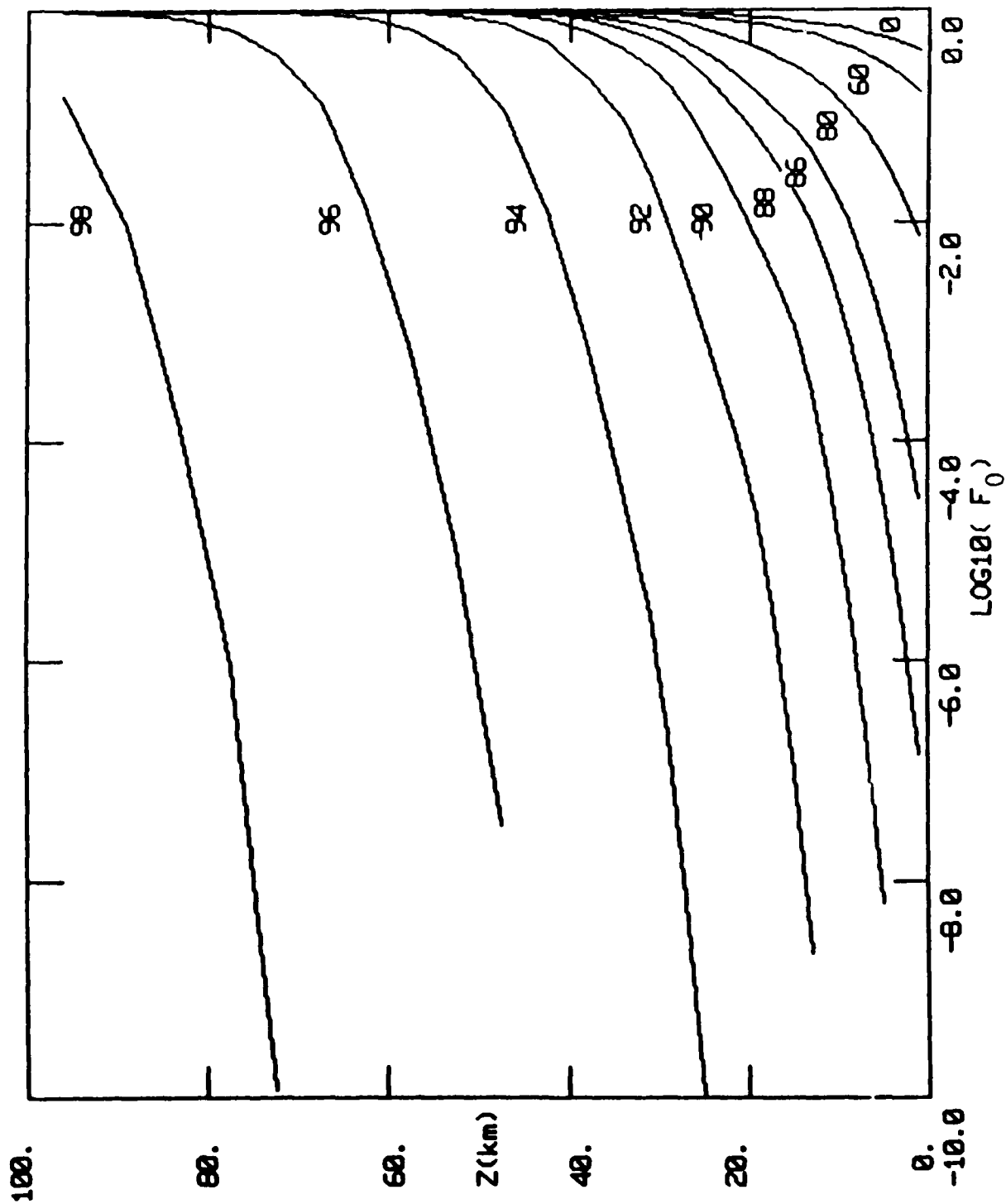


Figure 4. Spherical F_0 at $\lambda = 325$ nm and, θ_0 as indicated.

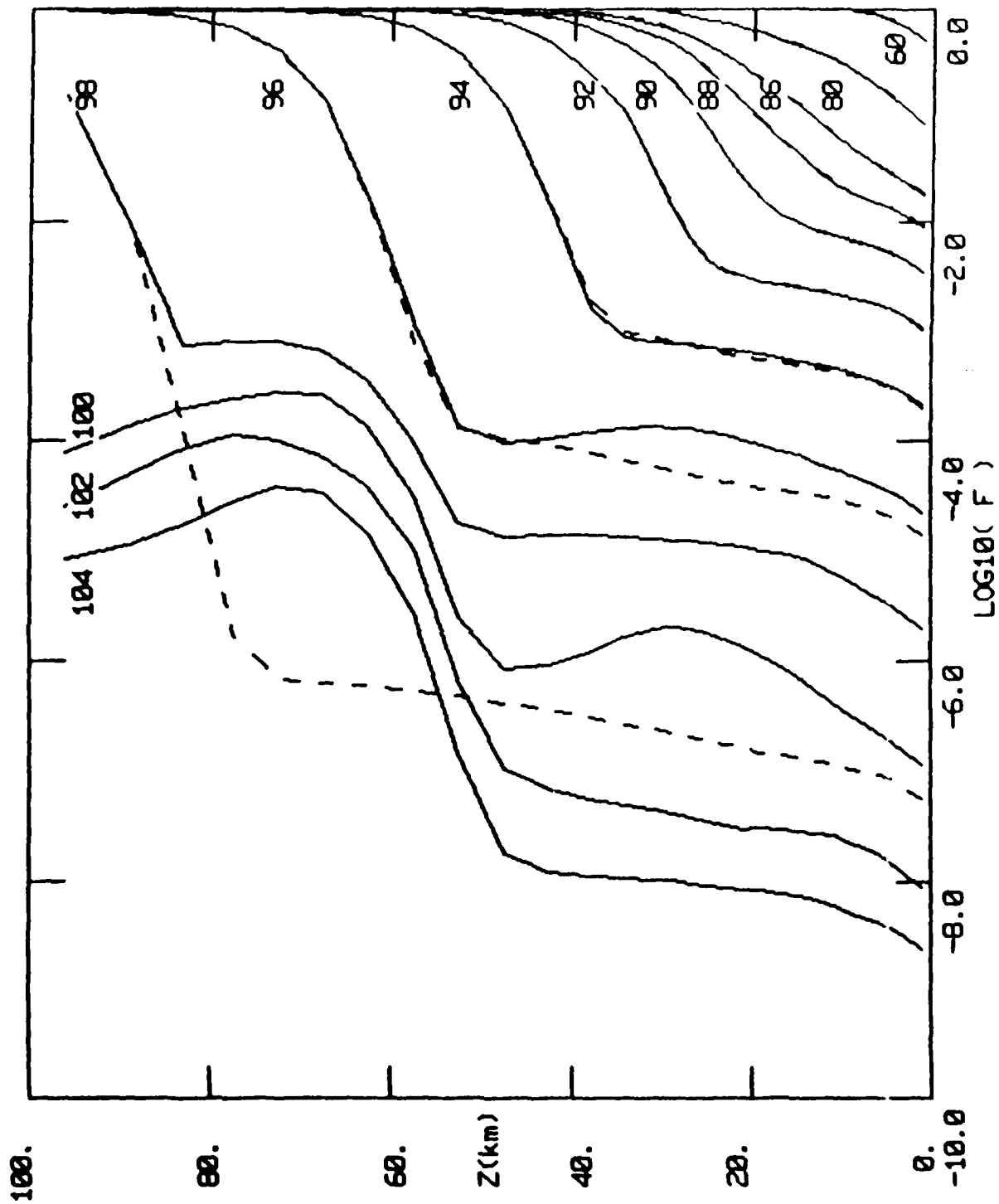


Figure 5. F as a function of O_0 at $\lambda = 325 \text{ nm}$. Solid curves are spherical solutions, and dashed curves are plane parallel solutions. C_0 as indicated.

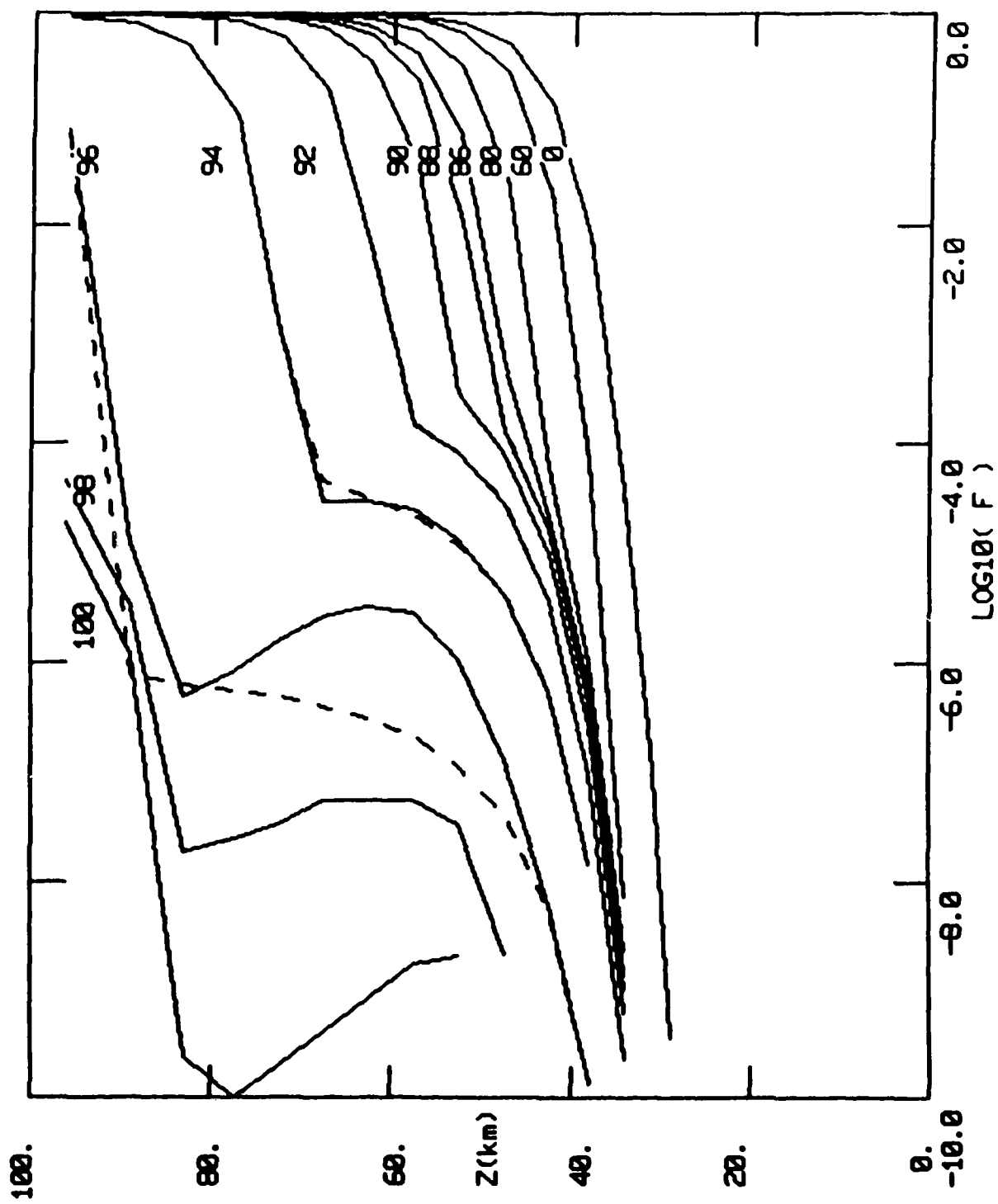


Figure 6. F as a function of θ_0 at $\lambda = 250 \text{ nm}$. See Figure 5 caption.

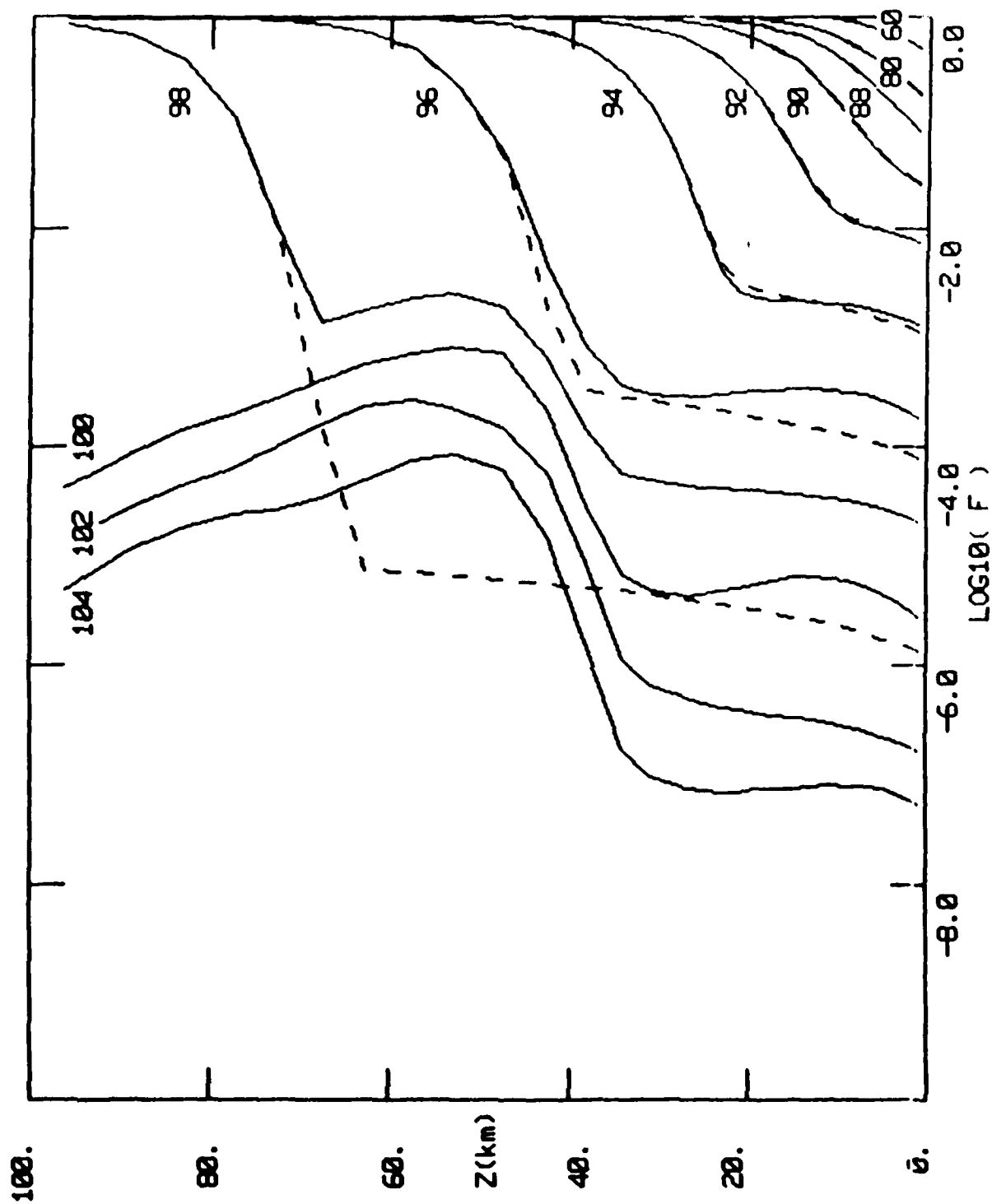


Figure 7. F as a function of O_o at $\lambda = 450 \text{ nm}$. See Figure 5 caption.

ATE
L MED
-83